

NPS ARCHIVE
1968
MORROW, G.

VISCO-ELASTIC DYNAMIC VIBRATION ABSORBER
GRANVAL L. MORROW
GEORGE A. CASLIR
PROFESSOR J.P. DENHARTOG
17 MAY 1968

Thesis
M8394

VISCO-ELASTIC DYNAMIC VIBRATION ABSORBER

by

GRANVAL L. MORROW
LIEUTENANT, UNITED STATES NAVY
B.S.E.E., PURDUE UNIVERSITY
(1961)

Submitted in Partial Fulfillment of the
Requirements for the Degree of
Naval Engineer and the Degree of
Master of Science in Mechanical Engineering

and by

GEORGE A. CASIMIR
LIEUTENANT, UNITED STATES COAST GUARD
B.S., UNITED STATES COAST GUARD ACADEMY
(1962)

Submitted in Partial Fulfillment of the
Requirements for the Degree of
Master of Science in Mechanical Engineering
and for the Degree of
Master of Science in Naval Architecture and
Marine Engineering

at the

MASSACHUSETTS INSTITUTE OF TECHNOLOGY

VISCO-ELASTIC DYNAMIC VIBRATION ABSORBER

GRANVAL L. MORROW

Submitted to the Department of Naval Architecture and Marine Engineering on 17 May 1968 in partial fulfillment of the requirements for the degree of Naval Engineer, and to the Department of Mechanical Engineering for the degree of Master of Science in Mechanical Engineering.

GEORGE A. CASIMIR

Submitted to the Department of Naval Architecture and Marine Engineering on 17 May 1968 in partial fulfillment of the requirements for the degree of Master of Science of Naval Architecture, and to the Department of Mechanical Engineering for the degree of Master of Science in Mechanical Engineering.

ABSTRACT

Objective:

The objective of this thesis work was the design, construction, and instrumentation of an apparatus to determine the dynamic properties of visco-elastic fluids for application in damped dynamic vibration absorbers.

Method:

The result of the design was a set of parallel plates tailored to fit a Calidyne #1500 shaker. The shaker was used to provide the driving force. The lower plate was held stationary and the upper plate constrained to move in one dimensional translation. The dynamic variables measured were the

magnitude of the applied force and phase angle between force and displacement. The force was measured via a strain gauge transducer, constructed for the thesis, and phase angle was measured by a phase detector using displacement as a reference. Both force and phase were plotted automatically against frequency by an X-Y recorder. The viscosity and modulus of elasticity were then calculated from the measured quantities.

Results:

The apparatus was shown to function satisfactorily and sufficient data was taken to check the performance with results obtained from the Caterpillar Tractor Company* for the silicone fluid used in the test. Both sets of data were shown to be in close agreement and not to follow linear visco-elastic theory, over the range of variables of interest. Both shear modulus and viscosity were found to be functions of frequency.

Conclusions:

It is the conclusion of the authors that this apparatus will perform satisfactorily for a wide range of fluids which may have damper application. The results will be improved, however, with implementation of the recommendations below.

* Data obtained via Professor J. P. DenHartog

Recommendations:

It is recommended that:

1. A device be designed to more accurately measure displacement.

The installed shaker metering is questionable at low frequency.

2. A suitably large two pen X-Y recorder be acquired such that force and phase may be recorded simultaneously.

3. A high input impedance D.C. differential amplifier be acquired for use with the strain guage bridge. The oscilloscope would then not be required, except for detailed wave form observations.

4. A relationship of the nondimensional coefficient to frequency and amplitude presented in this thesis be more thoroughly investigated.

If the variables are as simply related as the limited data indicates, the coefficient may prove a valuable analytical tool.

Thesis Supervisor: J. P. Den Hartog

Title: Professor of Mechanical Engineering, Emeritus
Professor of Naval Architecture and Marine
Engineering, Emeritus

ACKNOWLEDGMENTS

We wish to express our gratitude to our thesis supervisor,
Professor J. P. Den Hartog, for his inspiration and guidance.

To the following people for their technical advice and discussions:
C. W. Christiansen, R. B. Melton, Jr., L. G. Kurzweil.

To the United States Navy and the Coast Guard for the opportunity.

To our wives and families for their patience and tolerance.

TABLE OF CONTENTS

	page
TITLE PAGE	
ABSTRACT	i
TABLE OF CONTENTS	v
LIST OF FIGURES	1
LIST OF SYMBOLS	2
I. INTRODUCTION	3
II. PROCEDURE	5
III. RESULTS	6
IV. DISCUSSION OF RESULTS	20
V. CONCLUSION AND RECOMMENDATIONS	26, 27
VI. APPENDIX	
A) detail procedure and discription of apparatus	29
B) summary of data and calculations	33
C) supplementary notes for user of apparatus	39

LIST OF FIGURES

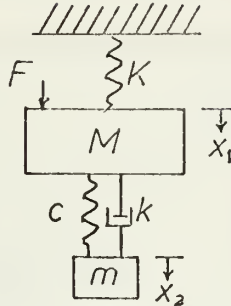
Figure	Title	Page
1.	Apparatus	8
2.	Interconnecting diagram	9
3.	Force vs. frequency, dry run	10
4.	Spring rate vs. frequency	11
5.	Damping coefficient vs. frequency	12
6.	Spring rate vs. frequency	13
7.	Modulus of elasticity in shear vs. frequency	14
8.	Dynamic viscosity vs. frequency	15
9.	$G/u\omega$ vs. frequency	16
10.	$G/u\omega$ vs. amplitude	17
11.	Stationary plate specifications	18
12.	Moving plate, rail and clamp specifications	19

LIST OF SYMBOLS

<u>Symbol</u>	<u>Meaning</u>	<u>Units</u>
A	Area of plates	(in ²)
c	Damping constant	($\frac{\text{lb.} \cdot \text{sec.}}{\text{in}}$)
e	Voltage	(volts)
f	Frequency	(hertz)
F	Driving force vector	(lb)
F _d	Damping force	(lb)
F _s	Spring force	(lb)
F _I	Intertial force	(lb)
G	Modulus of elasticity in shear	($\frac{\text{lb}}{\text{in}^2}$)
g	Forced frequency ratio	($\frac{w}{\omega_n}$)
k	Spring constant	($\frac{\text{lb}}{\text{in}}$)
M	Mass	(slugs)
m	Mass	(slugs)
η	Mass ratio	($\frac{m}{M}$)
μ, ν	Dynamic viscosity	($\frac{\text{lb} \cdot \text{sec}}{\text{in}}$)
ν	Viscosity kinematic	($\frac{\text{ft}^2}{\text{sec}}$)
w	Frequency	Radians/sec
x	Displacement	(in)
x _o	Peak displacement	(in)

INTRODUCTION

A damped dynamic vibration absorber consists diagrammatically as follows:



Where:

M is a large mass whose displacement x_1 we would like to minimize. This can be accomplished by the procedure of choosing the damper constants k , c and m , called tuning, (see reference 1, pp. 87-106). When this damper is physically applied to torsional systems, such as internal combustion engines, the spring required to take the displacement and cyclic fatigue are too large for practical application. At present, the compromise is to use a damper containing viscous or dry friction damping only. Reference 1 shows that this is a poor compromise, at best, in terms of the ratio of mass of the engine to mass of the damper. In diesel engine design the weight problem is most critical. In addition, the work/cycle done in dissipating the unwanted vibrations are considerably less in the friction dampers than the tuned damper (see Reference 1, pp. 101). Both of the above result in over design of crank shafts etc. to withstand the vibration.

This, then, is the motivation for thesis, to build a test apparatus to investigate visco-elastic fluids for their use in damped dynamic vibration absorbers. As the name implies, these fluids possess spring-like properties

as well as viscous effects, and if these are of sufficient magnitude, they should find wide application.

As shown in Reference 1, the ratio of spring force to damping force is a function of mass ratio and force frequency for optimum damping.

$$\frac{k}{c\omega} = \sqrt{\frac{2/3}{\eta(1+\eta)}} \frac{1}{g}$$

A representative range is:

$$\begin{array}{ll} \eta = 0.2 & \frac{k}{c\omega} = 1.67 \quad * \\ \eta = 0.01 & \frac{k}{c\omega} = 8.15 \end{array}$$

The problem then is to design and construct a machine to measure k and c (or G and μ) of the many visco-elastic materials now available. The difficulty, however, is that both k and c are functions of frequency and amplitude. The result of this thesis is a machine to measure $k(f, x_0)$ and $c(f, x_0)$.

*see non-dimension coefficient pp.

PROCEDURE

Design: Preliminary Considerations

Translational motion was chosen for the mode of operation primarily because of the availability of the calidyne #1500 shaker as a driving force.

The pertinent features are:

1. Three methods of operations, i.e. constant displacement (x), velocity ($w x$), or acceleration ($w^2 x$), each independent of frequency. This aids greatly in parameterizing the results.
2. The shaker is instrumented such that these variables ($x, wx, w^2 x, f$) can be read directly or use made of voltage outputs proportional to these variables. This simplified the instrumentation problem.
3. The shaker has frequency scan mode such that the data may be recorded swiftly and maintained near isothermal conditions in the fluid.

The size of the fluid contact area of the plates (10" x 12") was motivated by previous experience of Catapillar Tractor Company. This area provided sufficient measurable voltages at the strain gauge bridge. (See Appendix A for details).

Aluminium was chosen as the plate material because of ease of machining (See Figure 1 for configuration).

RESULTS

A. Figure 1 shows the result of the machine design. The key is as follows:

1. Shaker attachment plate threaded to receive transducer.
2. Transducer. Four active strain gauges, type BLH CB-10 isoelastic wire grid.
3. Moving plate with four lightening depressions (for mass reduction). Lower surface milled to fit into stationary plate well.
4. Six pressure clamps, with ball bearings installed in the notches, to prevent vertical motion and maintain clearance at a low friction level.
5. Battery and terminal box for strain gauge bridge.
6. Stationary plate.
7. Fluid well (0.100 inches deep).
8. Two bearing rails showing ball bearings.
9. Shim for clearance adjustment.
10. Bearing rail slot.
11. Two stationary plate constraint brackets to hold plate solidly to shaker.
12. Brace.

B. Figure 2 - interconnecting diagram. Connections and circuitry from

strain gauges and battery are made through the terminal box shown in Figure 1. Annotation "e" means voltage proportional to.

- C. Figure 3 shows dry run friction test results. Acceleration was measured and inertial force calculated. The measured force and calculated inertial force are as shown. Frictional forces were assumed to be zero.
- D. Figure 4 - measured spring rate
- E. Figure 5 - measured damping coefficient.
- F. Figure 6 shows the effect of heat generation in fluid on the spring rate.
- G. Figure 7 - comparison of thesis and Caterpillar data for modulus of elasticity in shear.
- H. Figure 8 - comparison of thesis and Caterpillar data for dynamic viscosity.
- I. Figure 9 - nondimensional coefficient $\frac{G}{uw}$ vs. frequency.
- J. Figure 10 - nondimensional coefficient $\frac{G}{uw}$ vs. amplitude.

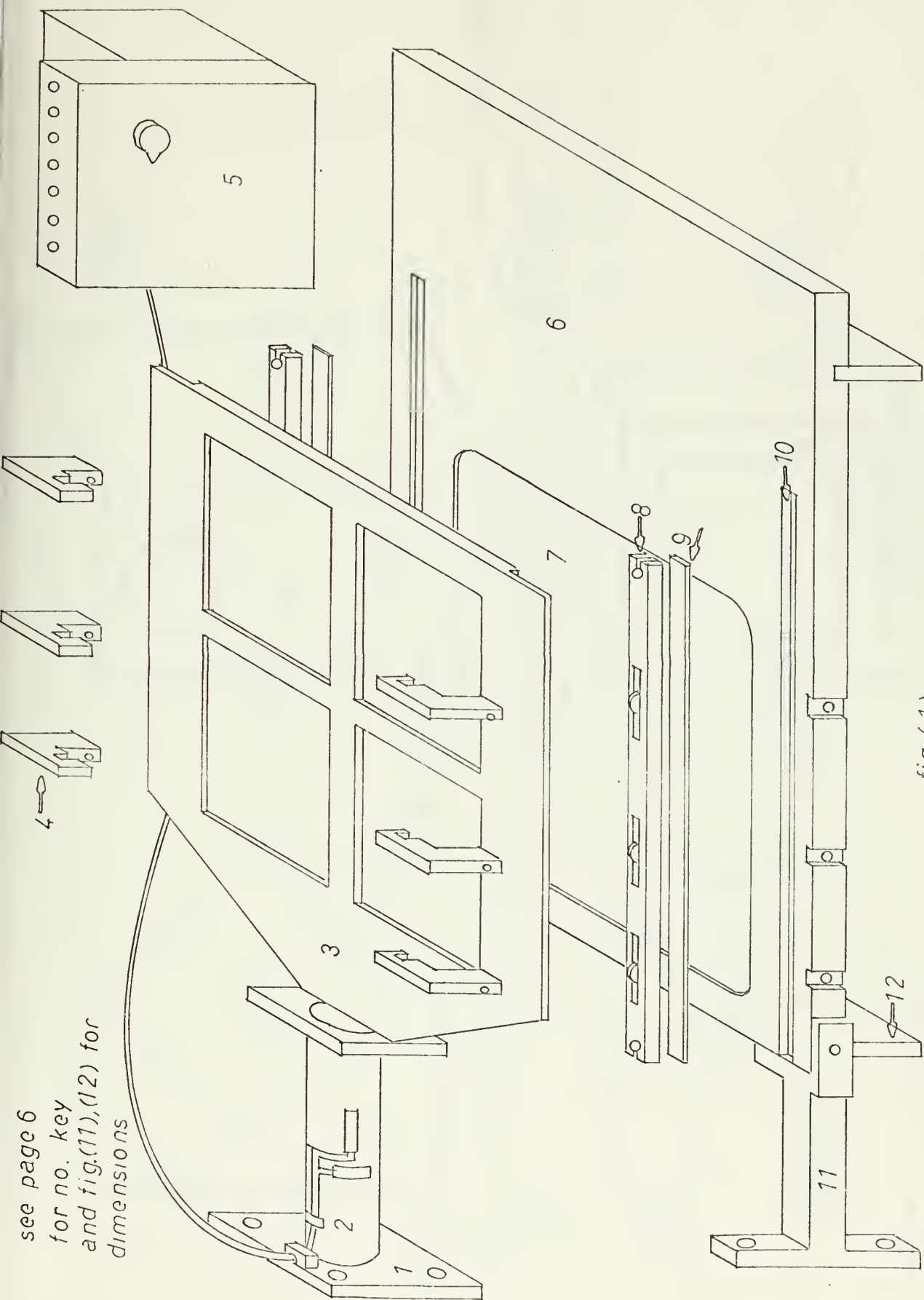


fig. (1)

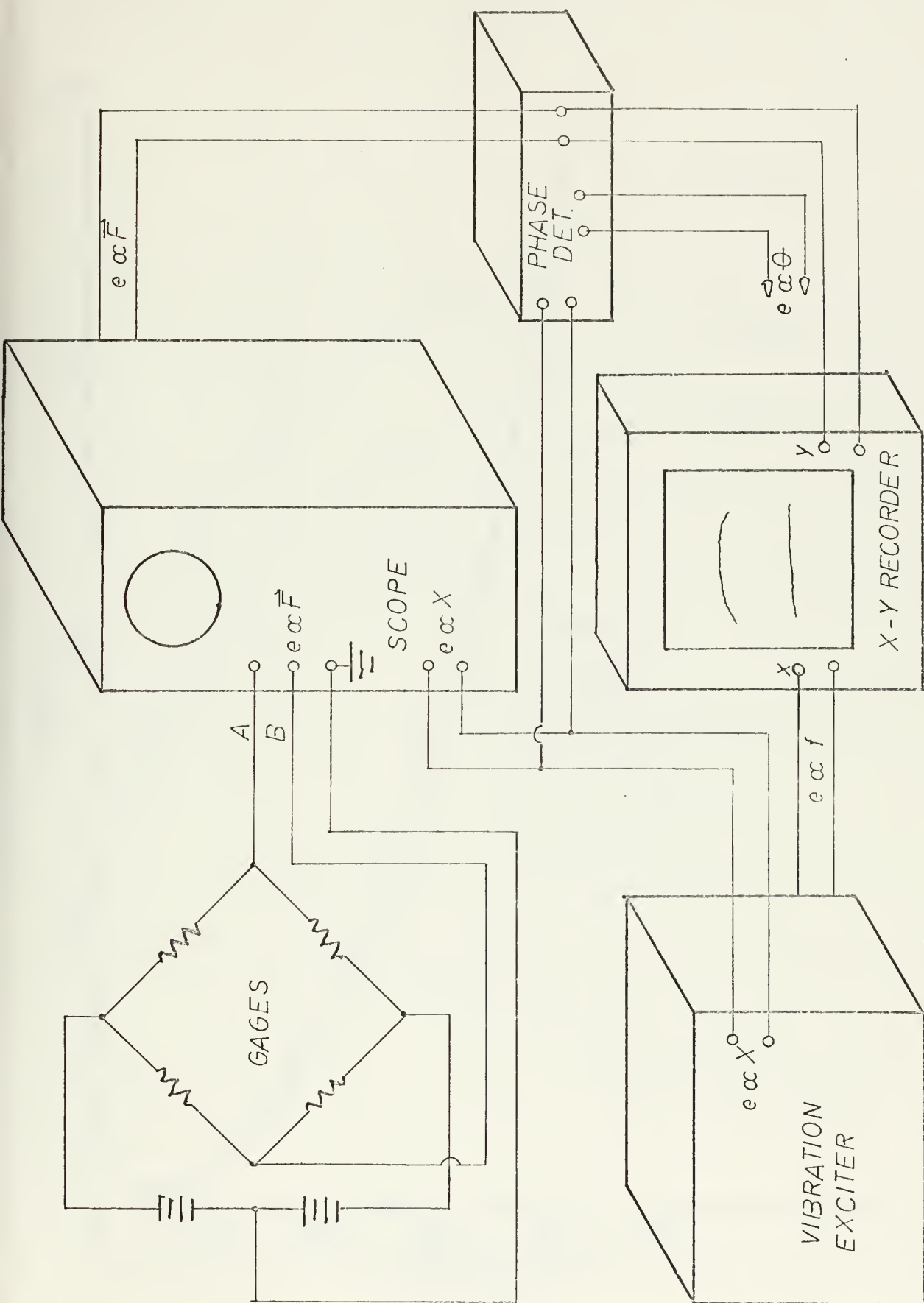


fig.(2)

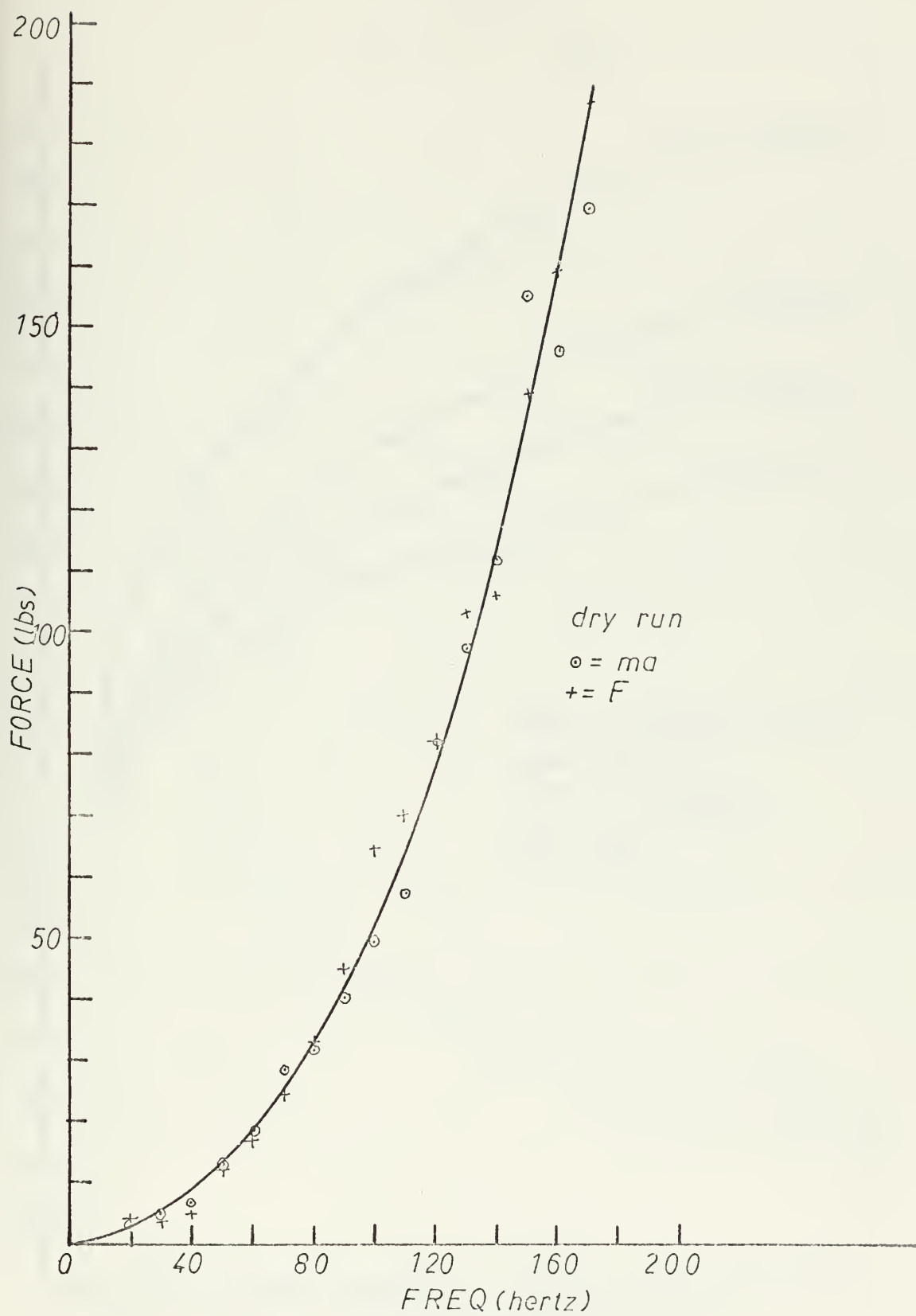


fig. (3)

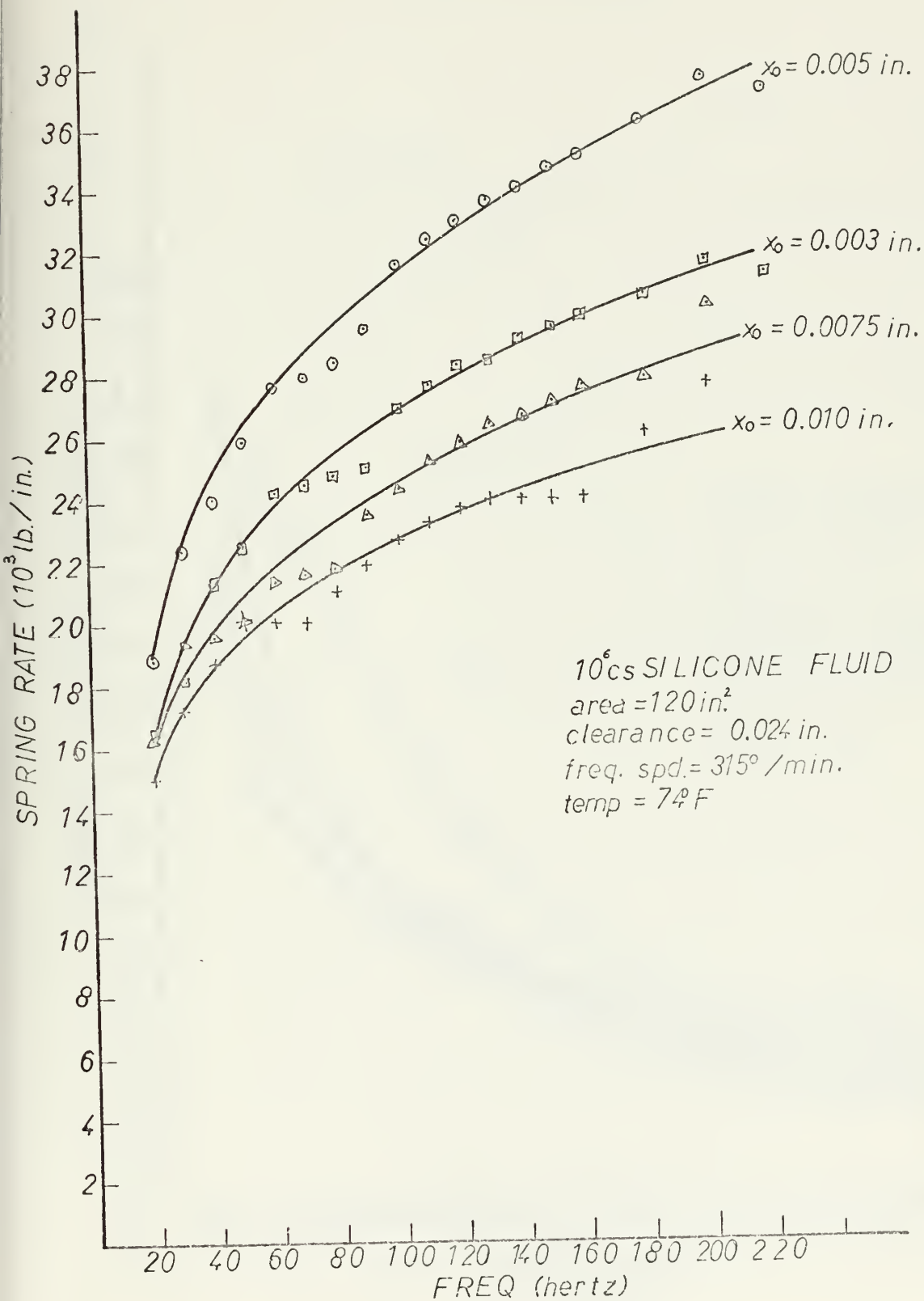
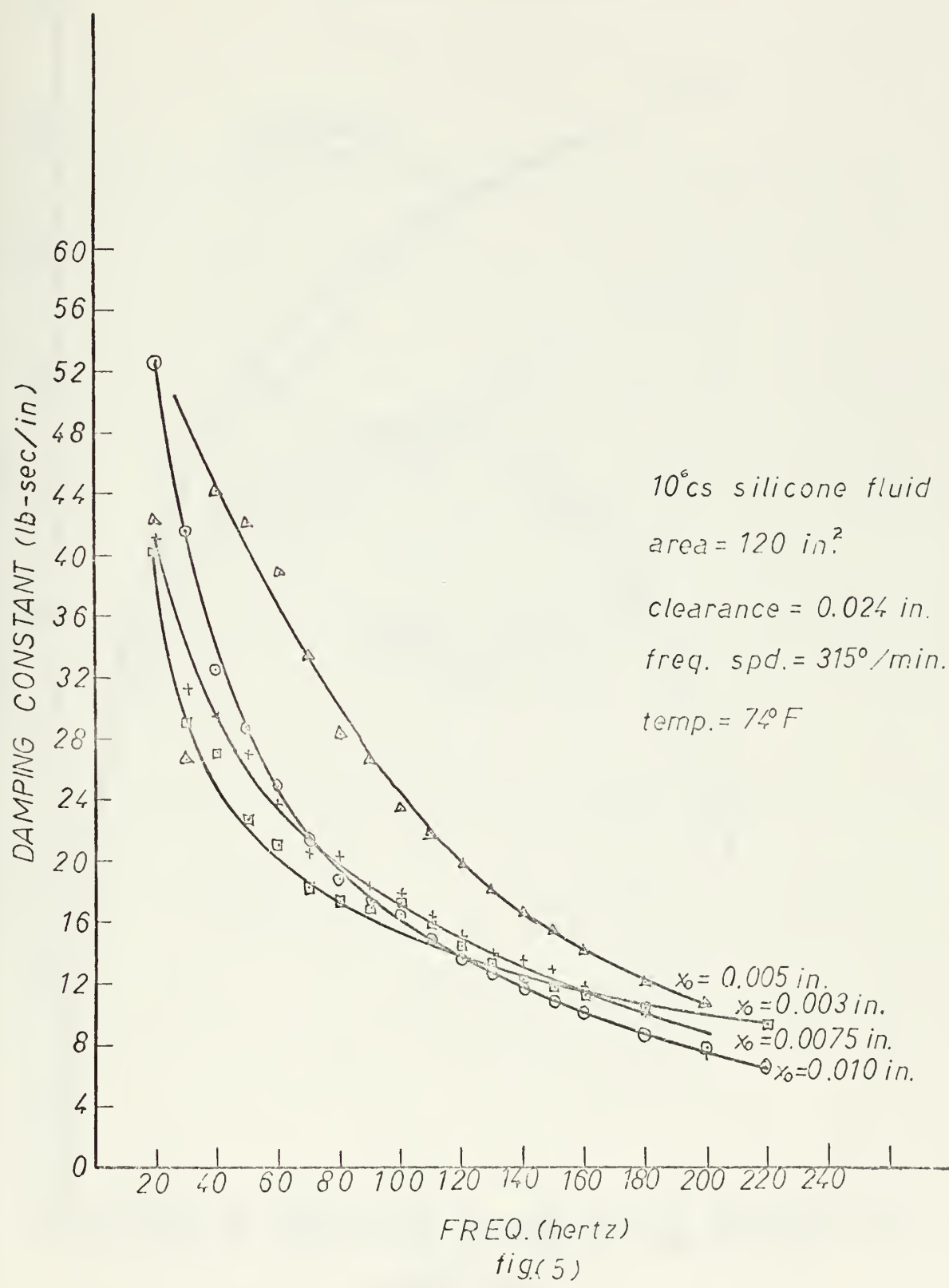


fig. (4)



10^6 cs SILICONE FLUID
 area = 120 in.²
 amplitude = 0.005 in.
 clearance = 0.024 in.

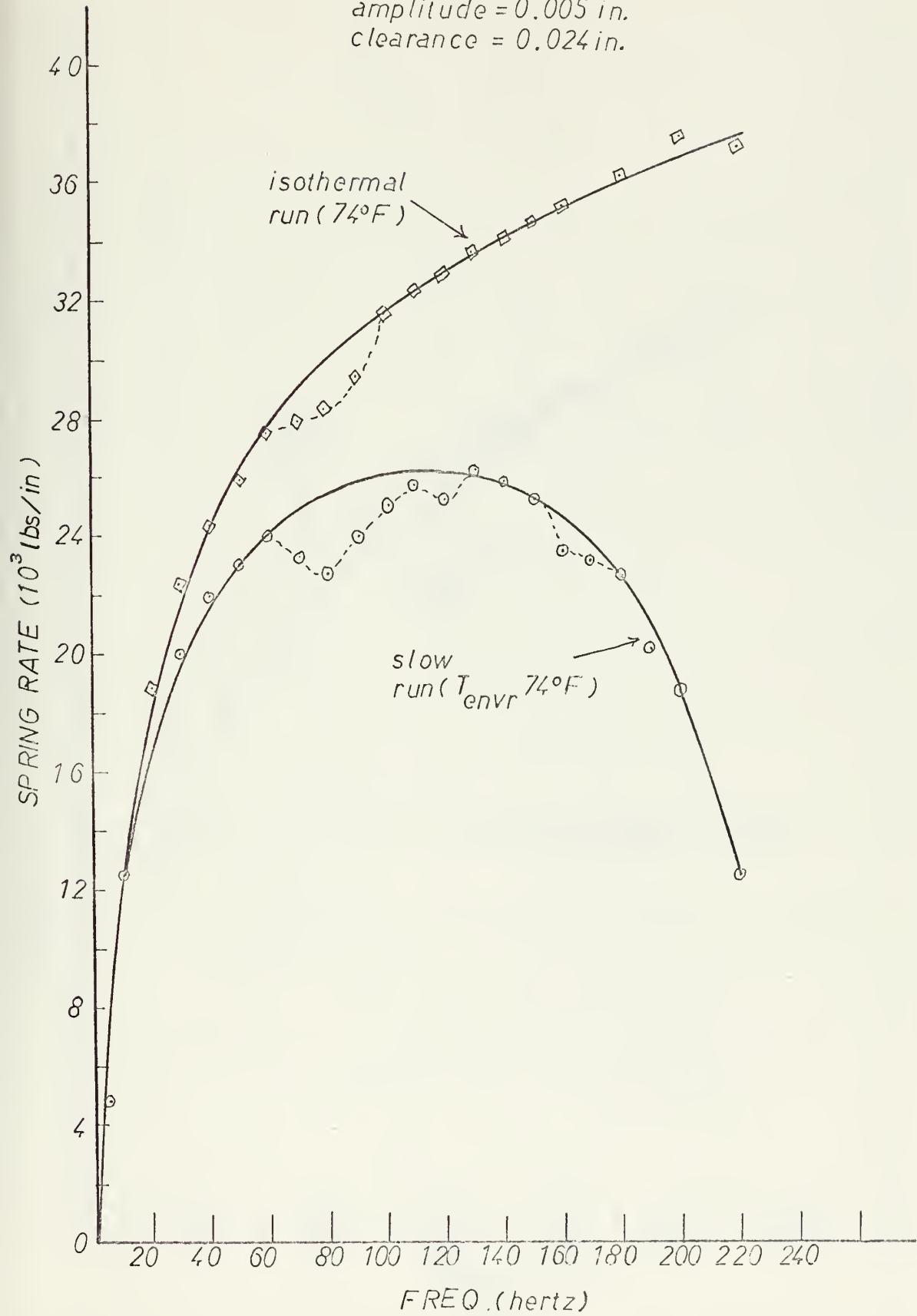
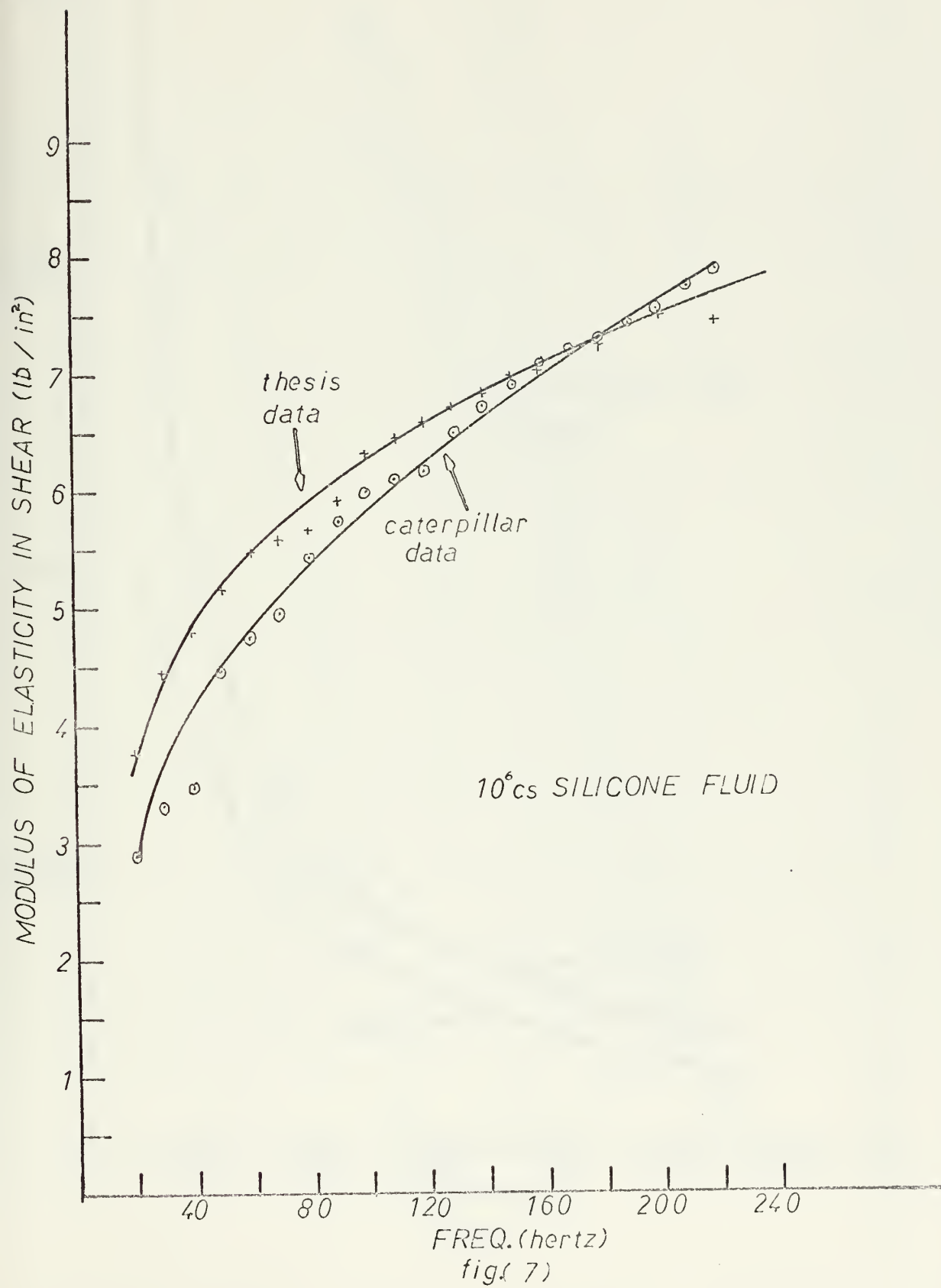


fig.(6)



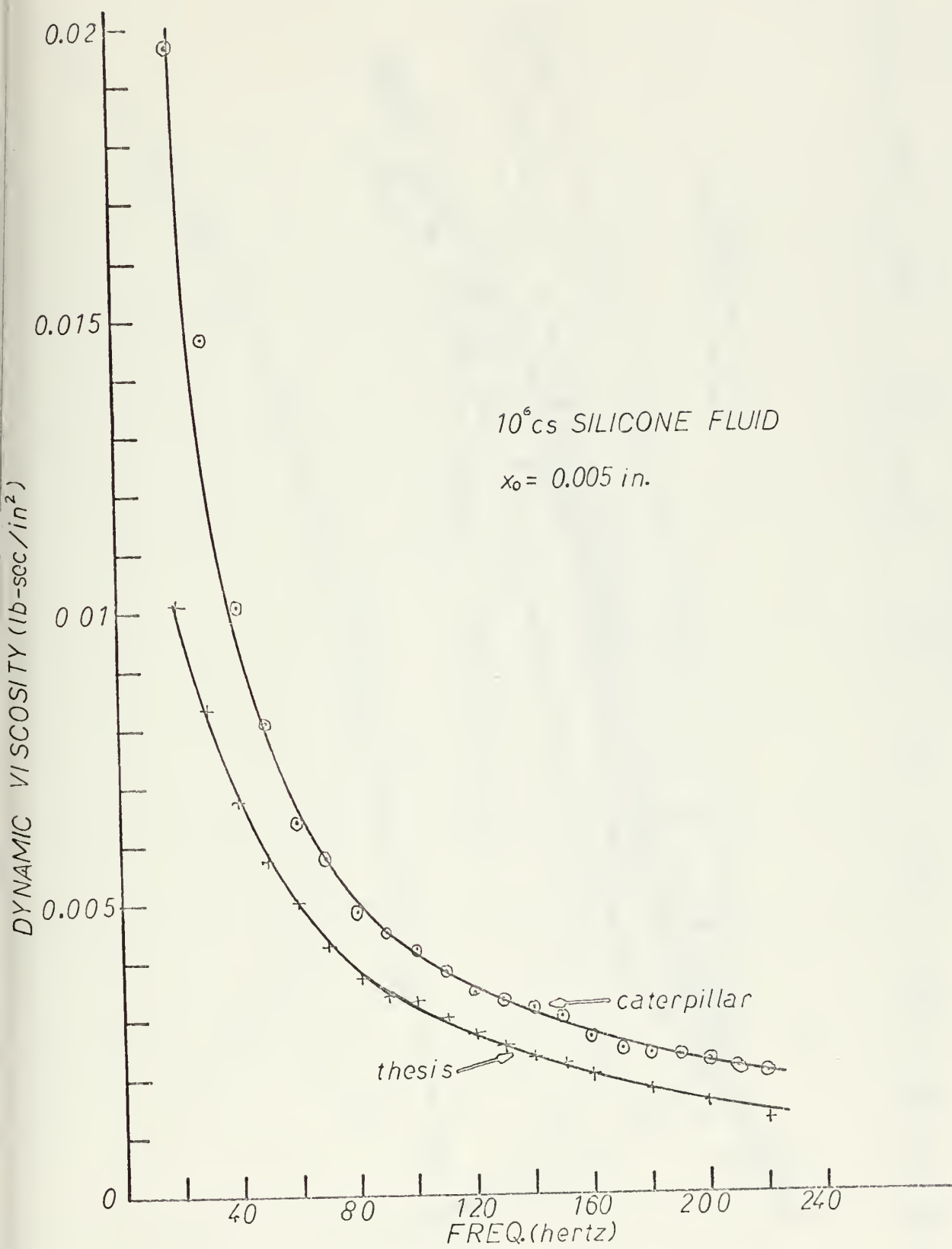
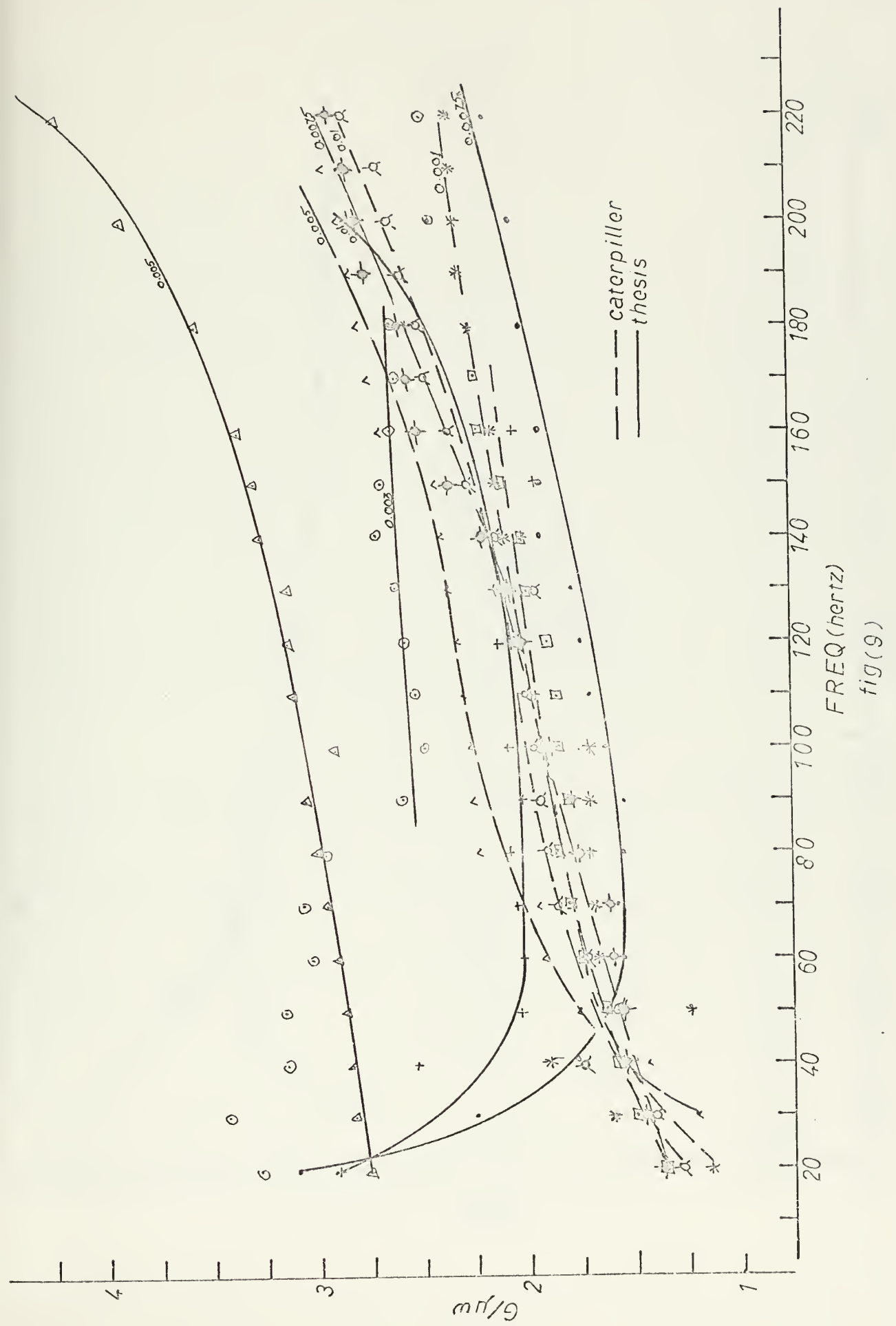
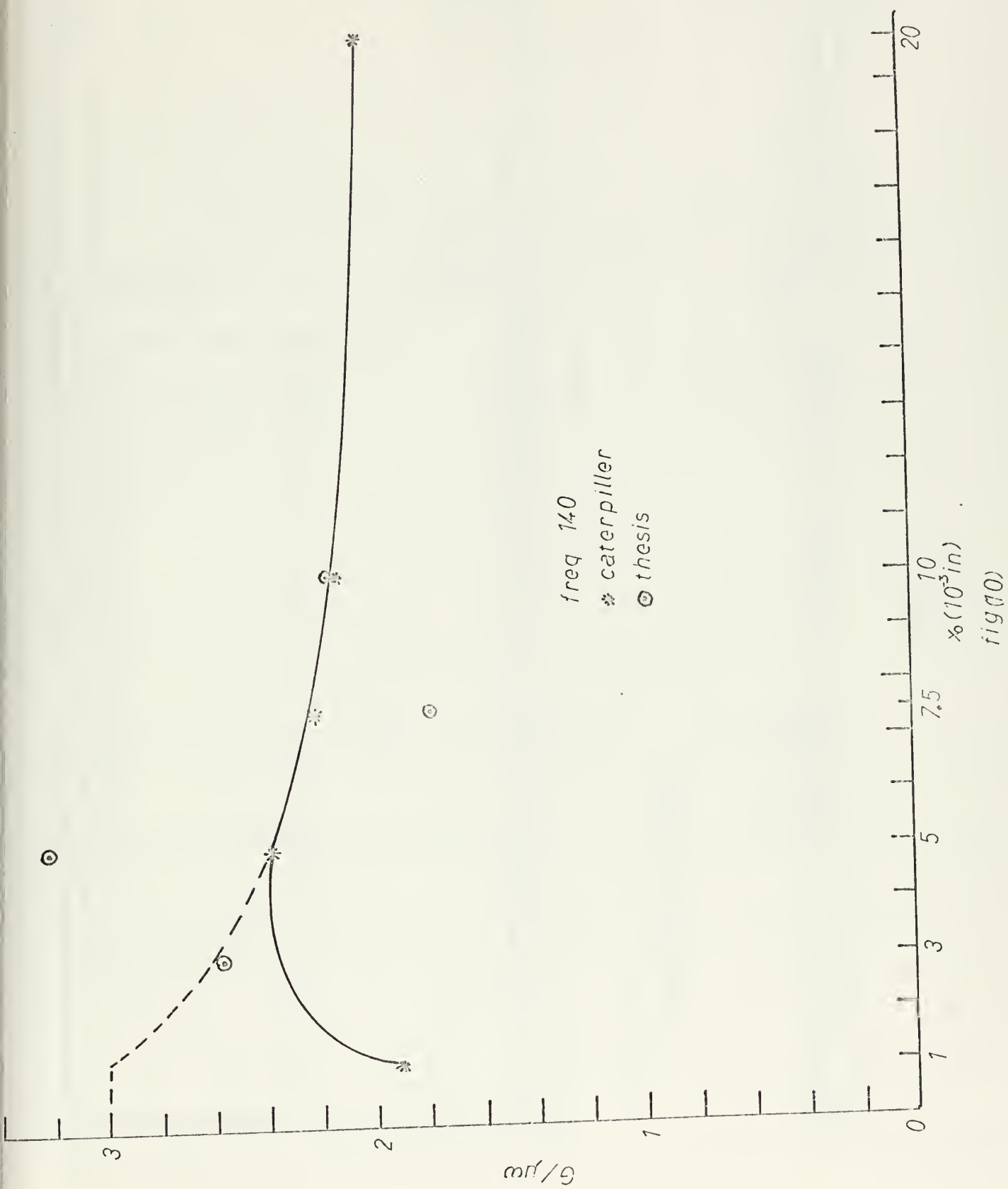
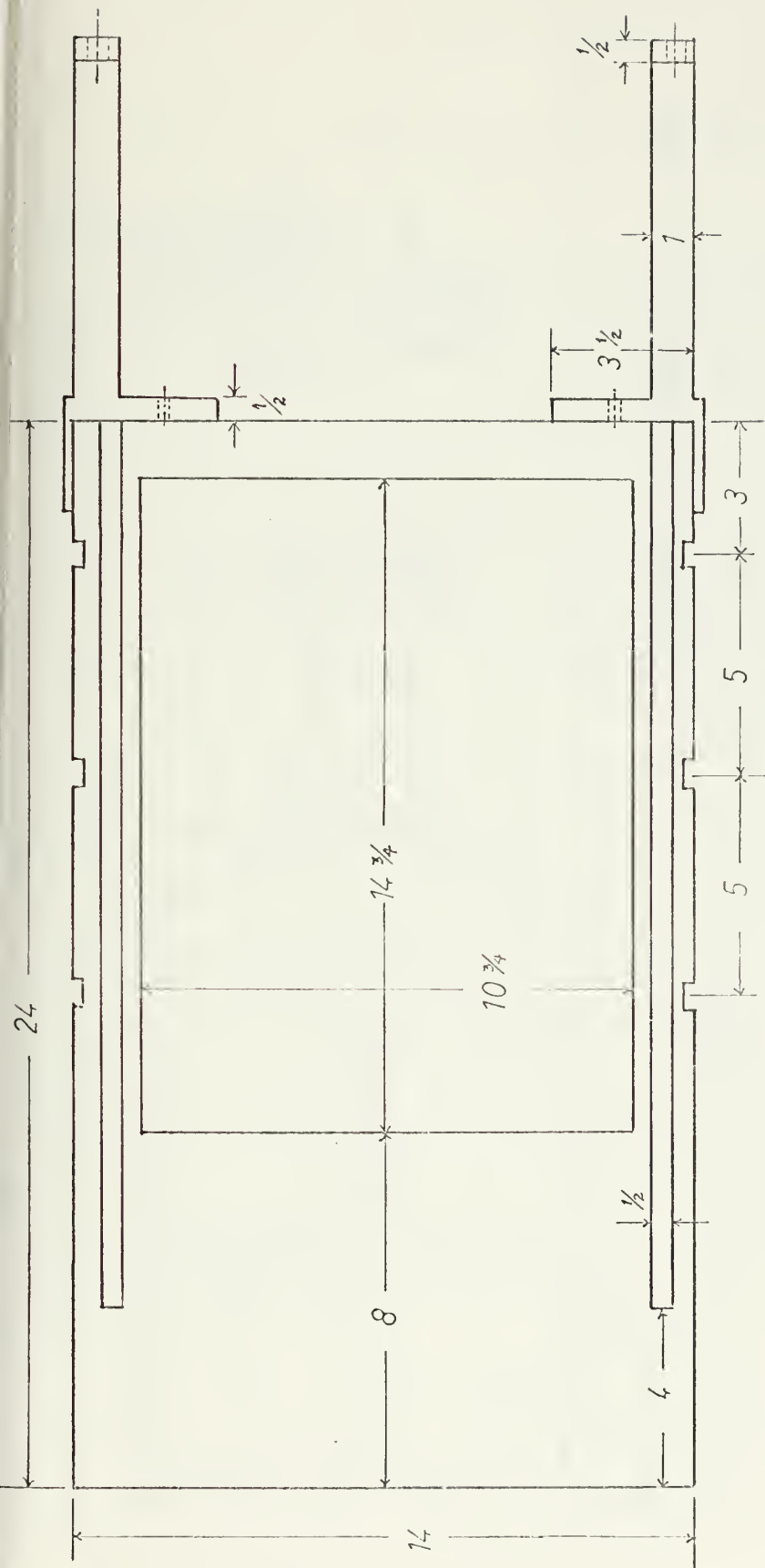


fig.(8)







dimensions in inches

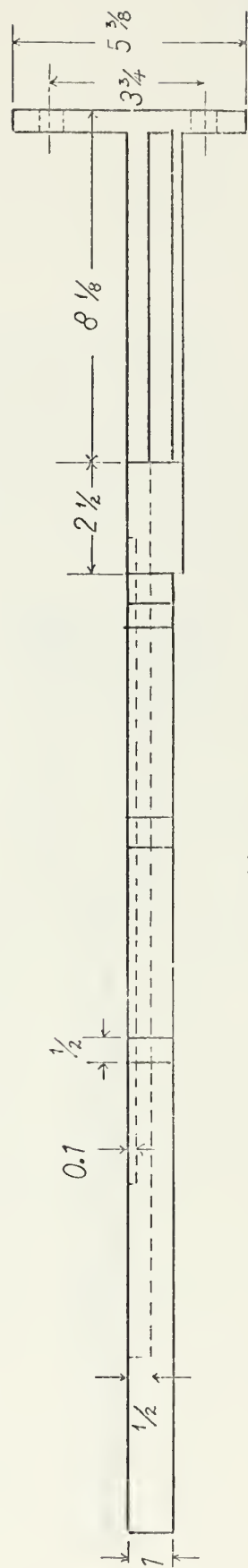


fig (11)

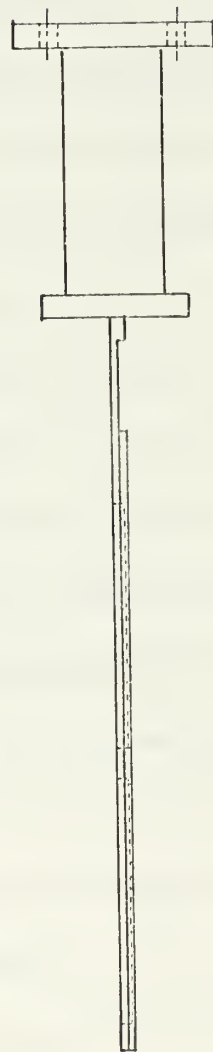
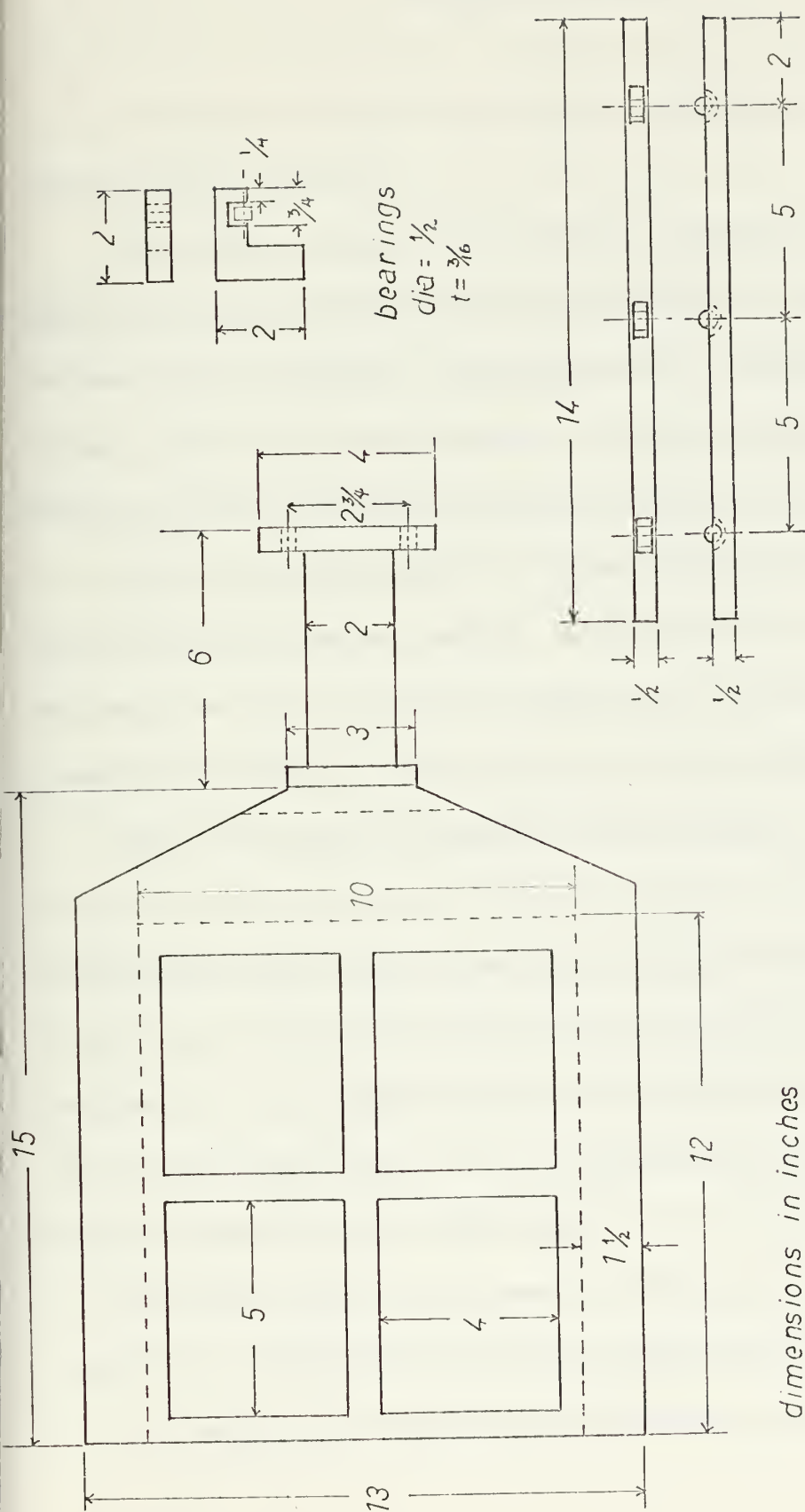


fig (12)

DISCUSSION OF RESULTS

The apparatus functioned as it had been designed to do. The following are significant highlights.

The transducer functioned excellently. Detailed observations of the force wave form indicated no apparent nonlinearity and equal amplitude both in tension and compression. Comparison with a standard load cell indicated virtually 100% strain gauge bonding. It is felt that strain gauge failure from fatigue will not be a problem, because the strain level is very low.

No serious buckling modes of vibration of the upper plate were noted with the pressure clamps installed. Some early data was obtained prior to lightening the plate. A comparison with results taken after showed no detectable change in the data, other than a decrease in the inertial force.

The instrumentation arrangement finally decided upon was the result of several attempts to obtain the desired information in its simplest and most readily useable form, and the fact that instrument capability was a very influential factor. The output of the strain gauge bridge is a double ended arrangement and it is not compatible with the single ended input required by the recorder and the phase meter. A D.C. differential amplifier was required and was only available on the oscilloscope.

The experimental results were in general agreement with the results obtained by the Caterpillar Tractor Company (See Figures 7 and 8).

The spring rate and damping coefficient are shown in Figures 4 and 5.

At a specific frequency both sets of data showed an increase in both the spring rate and the damping coefficient, peaking at about 0.005 inches displacement and then decreasing. This behavior is yet unexplained. The same result, but to a lesser degree, appears in the Caterpillar data.

It was noted that the initial results - Figure 6 - didn't conform to the expected results. It was found that the spring rate was highly temperature sensitive. To overcome this problem, one of two avenues of attack could be utilized. The best method was to take the data rapidly, using an X-Y plotter to record the force and phase angle automatically. Or, if this equipment was not available, the more tedious method of taking the data at a desired point stopping the shaker and allowing the fluid to return to thermal equilibrium then going on to the next point. Needless to say, this could take some time and no doubt any information obtained could be questionable. Another alternative would be the cooling of the plate by forced means to remove the heat generated by the damping of the fluid.

Note should be taken of the consistent dip in the spring rate between 60 cps and 100 cps, (see Figures 4 and 7). This occurred in both Caterpillar's and the thesis data. The significance of this was not determined.

Figures 9 and 10 show the results of plotting the data as a nondimensional coefficient as a function of frequency and amplitude. The nondimensional coefficient $\frac{G}{w u}$ was chosen for this purpose. This was chosen because it is the ratio of elastic force to damping force used in dynamic damper tuning and because of its direct relationship to the relaxation time (λ) used

by rheologist to describe the fluid, ($\lambda = \frac{\mu}{G}$). From the linear theory of visco-elastic fluids in steady state harmonic shear, the force equation is as follows:

$$F/A = \frac{u \lambda_0 x_0 w}{a(1 + \lambda_0^2 w^2)} \left[\frac{1}{\lambda_0} + jw \right], \quad w \ll \frac{\pi V}{a^2}$$

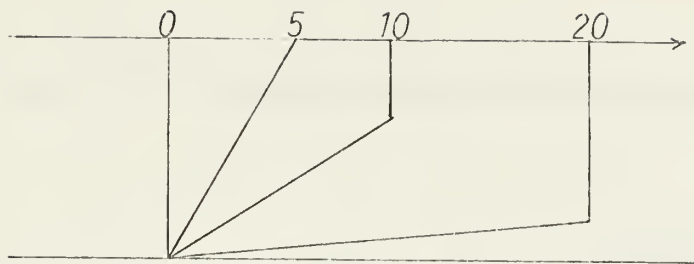
where a plate separation
 w frequency
 F magnitude of the applied force
 x_0 displacement at the moving plate
 A area of plate

The ratio of elastic to damping force is then:

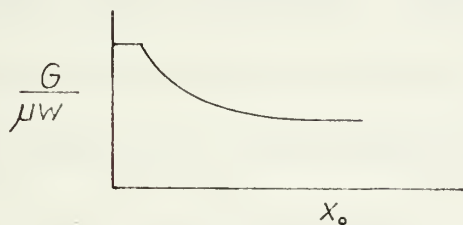
$$\frac{F_s}{F_d} = \frac{1}{w \lambda_0} = \frac{G}{w \mu}$$

λ (or $\frac{\mu}{G}$) is not constant with frequency or amplitude in the real fluid. However, the experimental data indicates a simple relationship for $\frac{G}{w \mu}$ v.s. freq. and some convenient information can be obtained from the $\frac{G}{w \mu}$ v.s. amplitude plot. (See Figure 9 and Figure 10). Figure 9 shows an almost linear relationship of $\frac{G}{w \mu}$ v.s. freq. for a constant amplitude. The data is considerably scattered at the low frequencies due in large part to error in the phase angle measurement. The trend in both the thesis and Caterpillar data is, however, strongly evident.

The explanation offered here for the behavior of $\frac{G}{w \mu}$ v.s. x_0 curve is based on the following simplified (overly perhaps) model at a constant frequency.



Between 0 and 3 the fluid follows the linear viscoelastic formulation and $\frac{G}{w u} = \text{constant}$. Above 3, the breaking and regeneration of bonds in the polarmeric material come to equilibrium and so the elastic energy stored becomes a constant. As the displacement increases, the process extends across the gap. The data indicates that the damping force is a very weak function of x_0 and it would follow $\frac{G}{w u} = \text{constant}$.



The argument above is based partly on the linear theory, partly on the data and partly on the physical model of the material structure. The conditions for linearity are that displacement and shear rate be small. The shear rate for example at $x_0 = 0.5 \times 10^{-3}$ inches and 100 cycles is:

$$\frac{w x_0}{a} = 13 \text{ sec}^{-1}$$

Reference 2 (pp. 149) states that shear rate is this neighborhood and below exhibit linear response. The point being that at some small displacement $\frac{G}{w u}$ should approach a constant as the linear theory predicts.

The second part of the argument, based on the data, is that the gentle

decrease from $5 - 20 \times 10^{-3}$ inches indicates a decrease in elastic stored energy since:

$$\frac{G}{\mu w} \propto \frac{\text{energy stored}}{\text{energy dissipated}}$$

Since c is a very weak function of x_0 , $\frac{G}{w u}$ will decrease with decreasing or constant elastic stored energy (energy dissipated $\propto w c x_0^2$). Assuming the above argument valid, how can the decrease in elastic energy be explained? A first order physical model of the fluid is that it is made of long chain molecules which may be stretched and store energy. These chains do break, however, and are in some spontaneous way regenerated. We have, then, two rate processes which must come to equilibrium. The number of bonds breaking depend on x_0 and the number regenerating depend on the number broken. If this be so, this process should start at moving plate and progress across the gap. When the process reaches the bottom plate, the elastic stored energy increases with displacement at a slower rate while the rate of dissipation continues unaffected. The result is $\frac{G}{w u}$ decreases with displacement. In summary, the slope of $\frac{G}{u w}$ vs. X_0 should be zero for $X_0 = 0$ and the function should decrease for large X_0 . Still unanswered is the reason for the peak at about 0.005 inches. Present data is insufficient to explain the behavior in this region. The dotted curve in Figure 10 is meant only to represent conjecture based on the argument above.

Disregarding data below 70 cps because of the inaccuracy of phase measurement at low frequency (the phase meter used was not intended for use below 100 cps), the non-dimensional coefficient appears to increase linearly

with frequency. This increase seems independent of displacement. This behavior conforms to the simplified model discussed above.

It was observed that at high frequencies and/or large displacements, air was drawn under the plate edges. The effect of this problem was not pursued. The advent of aeration was carefully avoided by remaining at low frequencies (under 250 cps), small displacements and a large clearance. An investigation of this problem should be conducted using a transparent plate.

CONCLUSIONS

- 1) The apparatus functioned as desired.
- 2) The fluid did have sufficiently strong spring rate and damping coefficient to be useful in damped dynamic vibration absorbers.
- 3) The nondimensional coefficient may prove to be a valuable analytical tool if the fluid characteristics were investigated in depth.

RECOMMENDATIONS

- 1) Devise a more accurate method of determining the displacement.
- 2) Use a large two pen X-Y recorder to record the data.
- 3) Use a high input impedance D.C. differential amplifier.
- 4) A more thorough investigation of the nondimensional coefficient be conducted.
- 5) Make a moveable plate from plexiglas to observe the advent of aeration and fluid separation and their effect on the results.
- 6) A more readily adjustable clearance control be devised.

APPENDIX

APPENDIX A

Detailed Procedures

1. The shaker control, the recorder and other associated equipment was calibrated and set to indicate force vs. frequency, and for the second run, to indicate phase angle vs. frequency. The runs were made at a constant displacement. The frequencies were scanned using this feature of the shaker controls.

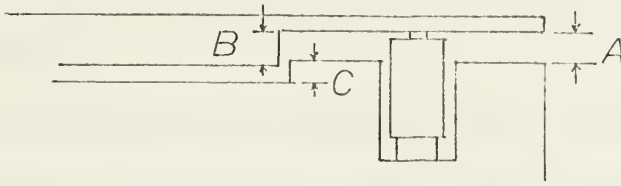
Each run was made at the same temperature. This was done to minimize the variation of the fluid properties with temperature.

The measured force is the absolute value of the vector sum of the inertial force of the plate, spring force and the damping force. The phase angle is the angle between the measured force and the velocity vector. The vector force can be solved for the spring force and the damping force, knowing the inertial force from calculation. From these forces, the spring and damping constants were determined.

The values determined were plotted against frequency and compared to the results obtained by Caterpillar. A comparison was also made of the shear modulus and the dynamic viscosity.

2. Determination of the plate clearance (thickness of the fluid).

The depth of the well and bearing rail slot, the thickness of the plate at the center portion and at the outside edge, the height of the bearing rail and the thickness of the shim were measured.



A = Shim + Rail & bearing height - Slot depth

B = Plate thickness - Edge thickness

C = Well depth

Clearance = $C - (B - A)$

3. The determination of the value or influence of frictional forces.

Frictional forces were reduced by using ball bearings as wheels on which the plate rolled. Considering the displacements involved and the minimal vertical loading of the plate, the frictional forces were thought to be negligible. A dry run (without fluid) was made through the frequency range in question. The inertial force was calculated and the loading on the transducer was measured. The results are shown plotted in Figure 3. Based on these results, the frictional forces were ignored.

4. Calibration of the strain gauge transducer.

The transducer was calibrated by unbalancing the bridge with a resistor. This unbalance was compared to a force that caused a similar unbalance. To observe this calibrated force a chopper was used to place a square wave on the transducer circuit. The wave-height on the scope and the displacement of the plotter represented a force of 63 pounds. This was done prior to each run.

5. Transducer Set-Up.

The transducer was made from a length of #40 2" aluminum pipe. The outside diameter was turned to concentricity with the inside diameter to the desired thickness. Four BLH SR-4 Type CB-10 were placed on the outside, two axially and two circumferencely (the pairs being placed opposite each other) in the standard Wheatstone Bridge. The Bridge was powered by a 45 volt battery.

6. Fluid Placement

Due to the high viscosity of the fluid, one runs into the problem of having to spread the fluid rather than waiting for it to flow. The fluid was spread over the area of the well and heated by lamps. It was allowed to stand overnight to insure smoothness and evenness of depth. It is recommended that the fluid be heated by infra-red lamps to enhance this process.

7. Well plate motion isolation.

The well plate was clamped to the shaker to prevent its movement due to forces transmitted through the fluid. The movement of the plate was checked with an accelerometer. Its motion, if any, could not be detected above the background noise of 0.1 g.

8. Instrument Calibration and Set-Up.

All equipment was set up and calibrated in accordance with their respective instruction manuals. No problems were encountered.

Equipment List:

- 1) Calidyne Model A174 Shaker

Calidyne Model 231 Control Panel

Calidyne Model 232 System Gain

- 2) Bruel and Kjoer Automatic Vibration Exciter Control

Type 1018

- 3) Tektronix Dual Beam Oscilloscope

Type 502A

- 4) Ithaco Amplifier

Model 255A

- 5) Endeveco Corp. Accelerometer

Model 2242

- 6) General Radio Company Vibration Calibrator

Type 1557-A

- 7) BLH SR-4 Wire Strain Gauges, CB-10, $1000 \pm$ ohms, $3.2 \pm 1\%$

Gauge Factor

- 8) Battery #5308

APPENDIX B

SUMMARY OF DATA AND CALCULATIONS

$X_0 = 0.01$ Temp. = 74°F

FREQ.	FORCE	ANGLE	DAMP FORCE	INERT FORCE	SPRING FORCE	K	C	G	u	G/uw
20	158	190	51.5	1.26	150.0	15.0	41.0	3.0	.821	2.90
30	180	19	58.7	1.88	172.3	17.2	31.2	3.45	.624	2.23
40	198	22	74.2	2.51	187.6	18.8	29.5	3.75	.592	2.52
50	210	22	78.6	3.14	201.0	20.1	25.0	4.02	.502	2.55
60	220	27	103.5	3.77	205.3	20.5	23.6	4.16	.548	2.02
70	219	27	103.0	4.39	207.7	20.7	20.5	4.154	.47	2.01
80	218	27	102.5	5.02	210.6	21.0	20.4	4.212	.408	2.05
90	222	29	104.3	5.65	218.9	21.9	18.4	4.37	.370	2.08
100	230	29	112.0	6.28	226.9	22.7	17.8	4.52	.357	2.01
110	229	29	111.0	6.90	231.8	23.2	16.1	4.64	.322	2.08
120	228	29	110.5	7.53	236.8	23.7	14.7	4.75	.322	1.96
130	225	30	112.5	8.16	238.7	23.9	13.8	4.78	.276	2.12
140	222	32	117.5	8.18	238.7	23.9	13.4	4.78	.268	2.03
150	220	35	120.5	9.41	238.2	23.9	12.8	4.76	.264	1.91
160	210	34	118.0	10.05	240.3	24.0	11.7	4.81	.235	2.03
180	202	29	177.0	11.30	260.7	26.1	8.7	5.214	.173	2.56
200	194	30	172.0	12.60	275.5	27.6	7.7	5.50	.165	2.83
220										

Temp. = 74°F

 $X_0 = 0.003$

FREQ	FORCE	ANGLE	DAMP FORCE	INERT FORCE	SPRING FORCE	K	C	G	u	G/uw
20	51.8	17	15.2	0.377	49.8	16.6	40.3	3.32	0.801	3.28
30	56.6	17	16.5	0.565	54.7	18.2	29.2	3.67	0.582	3.31
40	66.0	18	20.4	0.753	64.0	21.3	27.1	4.26	0.542	3.14
50	69.2	18	21.4	0.942	67.9	22.6	22.7	4.53	0.454	3.15
60	73.8	19	24.1	1.13	72.6	24.2	21.3	4.84	0.427	3.01
70	73.8	19	24.1	1.32	73.6	24.5	18.3	4.91	0.366	3.06
80	73.8	20	25.2	1.51	74.5	24.8	16.7	4.96	0.324	2.96
90	74.6	23	29.1	1.69	75.0	25.0	17.2	5.00	0.344	2.58
100	80.2	24	32.6	1.88	81.0	27.7	17.3	5.40	0.346	2.48
110	80.8	24	32.9	2.08	83.2	27.3	15.8	5.55	0.318	2.53
120	80.8	24	32.6	2.26	85.0	28.3	15.5	5.66	0.291	2.58
130	80.2	24	32.3	2.45	85.3	28.4	14.4	5.68	0.266	2.11
140	79.4	24	32.3	2.64	87.7	29.2	13.2	5.85	0.245	2.71
150	78.5	25	33.1	2.83	88.7	29.5	12.7	5.92	0.234	2.68
160	77.8	26	34.2	3.02	89.9	29.9	11.3	5.99	0.227	2.63
170										
180	75.4	28	35.4	3.99	91.7	30.5	10.4	6.12	0.209	2.59
190										
200	73.8	32	39.1	3.77	95.0	31.6	10.6	6.33	0.208	2.43
210										
220	67.7	34	37.9	4.14	93.7	31.2	9.16	6.24	0.183	2.47

Temp. = 74°F

 $X_0 = 0.005$

FREQ	FORCE	ANGLE	DAMP FORCE	INERT FORCE	SPRING FORCE	K	C	G	u	G/uw
20	99.0	19.5	33.1	0.628	93.8	18.76	52.7	3.75	1.06	2.76
30	118.0	19.5	39.4	0.944	112.2	22.44	41.8	4.46	0.835	2.83
40	125.0	19.5	41.9	1.29	120.0	24.00	32.5	4.80	0.672	2.84
50	133.5	19.5	44.8	1.57	129.2	25.84	28.6	5.16	0.572	2.87
60	141.0	19.5	47.1	1.88	137.7	27.54	25.0	5.47	0.500	2.90
70	141.0	19.5	47.1	2.20	139.3	27.86	21.4	5.57	0.429	2.95
80	141.0	19.5	47.1	2.51	141.3	28.26	18.75	5.65	0.375	3.00
90	145.0	19.5	48.4	2.83	147.5	29.50	17.10	5.90	0.343	3.04
100	154.0	19.5	51.4	3.14	157.9	31.58	16.35	6.32	0.328	2.90
110	155.0	19.5	51.7	3.46	161.6	32.32	14.95	6.46	0.300	3.11
120	155.0	19.5	51.7	3.77	164.6	32.92	13.70	6.57	0.274	3.16
130	155.0	19.5	51.7	4.08	167.9	33.58	12.65	6.72	0.253	3.25
140	154.0	19.5	51.4	4.40	170.4	34.08	11.65	6.83	0.234	3.31
150	153.0	19.5	51.1	4.72	173.1	34.62	10.80	6.92	0.218	3.36
160	151.0	19.5	50.4	5.05	175.1	35.02	9.98	7.00	0.207	3.36
170										
180	147.5	19.5	49.3	5.65	180.8	36.16	8.73	7.23	0.174	3.57
190										
200	144.0	19.5	48.1	6.28	187.7	37.54	7.66	7.50	0.153	3.90
210										
220	130.5	19.5	43.6	6.91	185.6	37.12	6.30	7.40	0.127	4.20

$X_0 = 0.0075$ Temp. = 74°F

FREQ	FORCE	ANGLE	DAMP FORCE	INERT FORCE	SPRING FORCE	K	C	G	u	G/uw
20	128	18°	39.6	.94	122.8	16.3	42.2	3.28	.841	3.10
30	151	18	46.6	1.42	145.8	19.4	26.6	3.09	.660	3.13
40	166	30	83.0	1.89	147.1	19.6	44.0	3.23	.882	1.77
50	177	34	99.0	2.36	151.8	20.2	42.0	4.05	.841	1.53
60	186	34	104.0	2.83	160.9	21.4	36.8	4.30	.738	1.54
70	185	34	103.5	3.30	162.5	21.8	31.4	4.34	.628	1.57
80	185	35	106.0	3.77	163.5	21.8	28.1	4.36	.564	1.54
90	192	36	113.0	4.24	176.7	23.5	26.6	4.62	.534	1.53
100	199	35	110.0	4.72	182.7	24.3	23.4	4.87	.477	1.62
110	200	34	112.0	5.18	189.5	25.2	21.6	5.06	.432	1.69
120	200	34	112.0	5.66	193.9	25.8	19.8	5.17	.397	1.73
130	199	34	111.0	6.12	197.8	26.4	18.2	5.27	.362	1.77
140	197	34	110.0	6.60	201.0	26.7	16.7	5.36	.334	1.87
150	193	34	108.0	7.07	203.7	27.1	15.3	5.43	.306	1.87
160	190	34	106.0	7.53	207.6	27.6	14.1	5.52	.282	1.94
180	185	34	103.5	8.48	209.0	27.8	12.2	5.57	.245	2.01
200	180	34	100.5	9.42	227.1	30.2	10.7	6.06	.214	2.16
220										

METHOD OF CALCULATION OF RESULTS

Spring Constant and Damping Constant Calculation

The measured force (F) is the absolute value of the vector sum of the inertial (F_I), spring (F_s), and the damping forces (F_d). The phase angle(θ) is the angle between the measured force and the displacement.

Force Eqn. steady state, harmonic motion

$$\begin{aligned} F &= -F_I + F_s + jF_d \\ &= -mw^2x_0 + kx_0 + jwcx_0 \end{aligned}$$

Inertial Force

$$F_I = ma = mw^2x$$

Spring Constant

$$F_s = kx = F \cos \theta + mw^2x$$

$$k = (F \cos \theta + mw^2x)/x$$

Damping Constant

$$F_d = xwc = F \sin \theta$$

$$c = F \sin \theta / xw$$

The weight of the place + half the weight of the transducer was taken as the total weight to compute the inertial force. The displacement was taken as indicated on the meter, after having checked its reliability by comparison of the measured and calculated force.

APPENDIX C

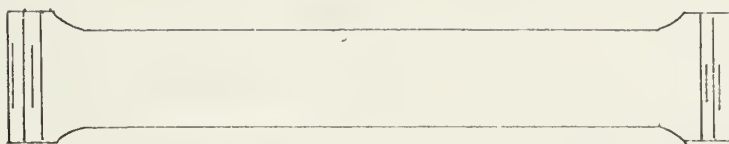
Summary: The diameter of the transducer pipe was chosen sufficiently large (2" nom.) so as to reduce the static strain placed on the strain gages. Calculation of the required cross sectional area was then made to suit the most severe of the flowing constraints based on a design load of 1500 lb.

1. Max. strain (in/in) for the strain gages.
2. Yield point of the material in simple compression.
3. Considering the pipe as a eccentricially loaded column.
4. Bending in a horizontal plane. (Motion is prevented by clamps and rails in a vertical plane.)
5. Buckling.

Bending was found to be the controlling factor and the resulting area was 0.385 in² for a factor of safety of 5.

Note should be taken here that the design load of 1500 lb is the maximum load that can be presented to the magnetic field of the armature before the shaker overloads. The armature inertial force must be subtracted from 1500 lb to determine the maximum load on the transducer. The design then is quite conservative and the transducer pipe may be thinned down inside if more bridge output is required.

Details:



Initial Pipe Data:

$$\begin{aligned}
 L &= 5.5" & I &= 0.666 \text{ in}^4 \\
 A &= 1.075 \text{ in}^2 & k &= 0.79 \text{ in} \\
 d_i &= 2.065" & \text{Material:} & \text{Al - alloy - 6061 - T6} \\
 d_o &= 2.375" & \sigma_{yp} &= 40,000 \text{ lb/in}^2 \\
 & & E &= 10^7 \text{ lb/in}^2
 \end{aligned}$$

Design load = 1500 lb

$$\sigma = P/A = \frac{1500}{A} = E\epsilon = 10^7 \epsilon$$

Max. ϵ for strain gage $1\frac{1}{2} - 2\%$, or 15,000 - 20,000 μ in/in (BLH Spec.)

Lower limit of area based on strain gage:

$$A = 0.00075 \text{ in}^2$$

$$\sigma = 2 \times 10^5 \text{ (beyond material } \sigma_{yp})$$

Lower limit of area based on σ_{yp} in compression only

$$A = .0375 \text{ in}^2$$

Lower limit of area for a short eccentrically loaded column.

(e = the inherent eccentricity, $\frac{ec}{R} = 0.6$)

$$A = \frac{P}{\sigma} \left(1 + \frac{ec}{k}\right) = 0.06 \text{ in}^2$$

In addition to the above, the transducer may be subject to bending in a horizontal plane due to off axis σ_{yp} (both static construction error and dynamic), and in the vertical plane due to off center loading. The fluid is below the $\frac{1}{4}$ in. plate.

e' for off center loading - $1/8"$

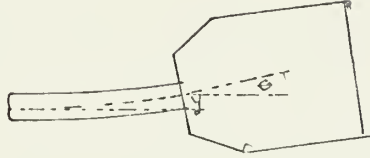
e' for construction (guess) - $1/16"$

e' for deflection in horizontal plane is handled as follows:

Deflection is assumed as that deflection caused by a bending moment that would strain the transducer to the elastic limit, or

$$\theta = \frac{Ml}{EI} \quad y = \frac{Ml}{2EI} \quad (\text{deflection due to moment at free end})$$

$$\sigma_{yp} = \frac{Mc}{I}$$

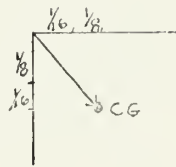


$$\text{Then } y = \frac{\sigma_{yp} l^2}{2cE} = 0.051$$

$$\theta = \frac{\sigma_{yp} l}{cE} = 0.00927, \quad x = 7.5\theta = 0.0696$$

We don't know for sure just how these will combine, but assume worst case or like this:

$$e' = \sqrt{(1/8 + 1/16)^2 + (1/16 + 1/8)^2} = 0.265"$$



$$\Delta = \frac{P}{\sigma_{yp}} \left(1 + \frac{ec}{k} + \frac{e'e}{k} \right)$$

$$\frac{e'e}{k} = \frac{0.315}{k}$$

We don't know what k is but we can take a conservative guess by using the last area calculated to find it since we know the inside diameter.

$$k = \sqrt{\frac{d_o^2 + d_i^2}{4}} \approx 0.73$$

$$A \approx \pi d_i t$$

$$t = 0.00925$$

$$d_o = d_i + t = 2.076$$

Then:

$$\frac{e'c}{k} = 0.431$$

$$A = 0.077 \text{ in}^2$$

$$\text{Assuming F.S.} = 5$$

$$A = -.385$$

$$d_o = 2.18''$$

Buckling:

(In compression)

$$\frac{L^2}{rt} = \frac{(8.5'')^2}{(.5)(.1)} = 245 \quad (\text{This is a long cylinder})$$

$$\sigma_{cr} = \eta CE t/r$$

$$t/r = 0.2 \quad C = 0.6 \quad \eta = 1 \text{ assumed, but close}$$

$$= (0.6) (10^7) (0.2) = 0.12 \times 10^7$$

(In bending)

$$\sigma_{crb} = C_B E t/r$$

$$C_B \approx 0.6$$

$$= 0.12 \times 10^7$$

$$\frac{\sigma}{\sigma_{cr}} + \frac{\sigma}{\sigma_{crb}} \leq 1$$

The material will fail in pure compress before any buckling for the above diminsions.

Requirements

1. High V and I . We are to measure very small stresses and $\Delta E \propto V$ which is limited by gage R . The bridge must generate ΔE_0 's great enough to be above oscilloscope amplifier noise. (about 20 μ volts).
2. High gage factor. Same reason as above.
3. The bridge need measure dynamic strain only.
4. Durable and long term stability. Apparatus to be used by students later.
5. Good electrical insulation from support be cause of high I .
6. Bonding must be fully effective because of small strains.
7. Should be functional to 200°C.

Selection

1. The criteria of high V, I, R , gage factor and dynamic strain dictates an iso-elastic gage.
2. Insulation, high I and temp. dictates a bakelite backing.
3. Temp., effectiveness and durability indicates an epoxy cement.

Gage Selected

BLM Electronics type iso-elastic wire

Grid - Bakelite base CB -10

$R = 1000 \pm 15 \Omega$ package tolerance
 ± 5

$S = 3.2$

$I_{max} = 50 \text{ M.A.}$

Size of grid $5/16 \times \frac{1}{4}$

Size of carrier $7/8 \times 3/8$

Cement - Eastman 910

Eastman 910 was selected because of its ease of application.

However, the operating temperature is limited to 200° w.

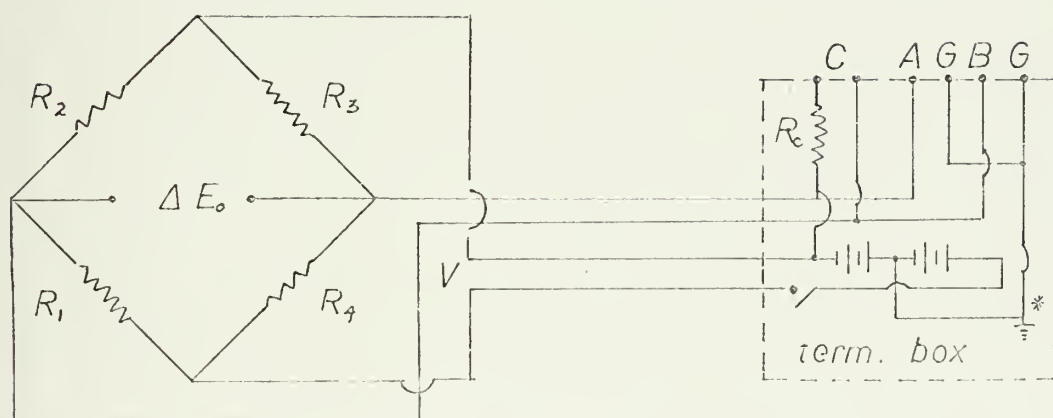
Surface Preparation

In accordance with M.I.T. strain gage lab instruction.

Bridge Design

The gages were attach such that R_1 and R_3 are longitudinal and

R_2 and R_4 are transverse. The resulting equations are as follows:



$$\Delta E_o = \frac{VSF}{2EA} (1 + \nu)$$

$$\eta = \frac{SF(1 - \nu)}{SF(1 - \nu) + EA} \quad (\text{non-linearity})$$

Where S = gage strain sensitivity (gage factor)

E = modulus

F = applied force

ν = poisson ratio

A = area

V = battery voltage

* This ground connection produces a zero static potential ΔE_o for a bridge made of perfectly matched gages. This was done to make the bridge voltages compatible to the input of the scope differential

amplifier. The maximum allowable static voltage input to the differential amplifiers is 2 volts on the lower millivolt scales.

Calibration

Calibration is accomplished by unbalancing the bridge with a known unbalance. The calibration resistor is placed across only one arm of the bridge. The calibration resistor used should have represented 96 lb in actual load. The actual value, however, was 126 lb when the bridge was checked against a std. load cell.

BIBLIOGRAPHY

1. Den Hartog, J.P., Mechanical Vibrations (New York: McGraw-Hill Book Company, Inc., 1947).
2. Fredrickson, A.G., Principles and Applications of Rheology (Englewood Cliffs, New Jersey: Prentice-Hall, Inc., 1964)
3. Eirich, F.R., Rheology - Theory and Applications, Vol. I, II, III (New York: Academic Press, Inc., 1956)
4. Reiner, M., Lectures on Theoretical Rheology (Amsterdam: North Holland Publishing Company, 1960).
5. Aronson, M.H., Nelson, R.C., Viscosity Measurement and Control (Pittsburgh, Pennsylvania: Instrument Publishing Company, Inc., 1964)
6. Dinsdale, A., Moore, F., Viscosity and Its Measurement (London: Chapman and Hall, Limited; New York: Reinhold Publishing Corporation, 1962)
7. Perry, C.C., Lissner, H.R., The Strain Gauge Primer (New York: McGraw-Hill Book Company, Inc., 1962)
8. Aronson, M.H., Nelson, R.C., Strain Gauge Instrumentation (Pittsburgh, Pennsylvania: Instrument Publishing Company, Inc., 1960)
9. Yarnell, J., Resistance Strain Gauges (London: Electronic Engineering, 1951)

thesM8394

Visco-elastic dynamic vibration absorber



3 2768 001 91726 3

DUDLEY KNOX LIBRARY